DEVELOPMENT OF AN EFFICIENT INSECT CONTROL SYSTEM BASED ON THE DOPPLER EFFECT

DAVID MACHARIA KIRIMA

MASTER OF SCIENCE

(Physics)

JOMO KENYATTA UNIVERSITY
OF
AGRICULTURE AND TECHNOLOGY

2022

Development of an Efficient Insect Control System Based on the Doppler Effect

David Macharia Kirima

A Thesis Submitted in Partial Fulfilment of the Requirements for the Degree of Master of Science in Physics of the Jomo Kenyatta University of Agriculture and Technology

2022

DECLARATION

This thesis is my original work and has not been submitted for a degree in any other university.

Signature…… Date……

David Macharia Kirima

This thesis has been submitted for examination with our approval as the university supervisors.

Signature…… Date……

Dr.-Ing. Kiroe Anthony, PhD

JKUAT, Kenya

Signature…… Date……

Dr. Ominde Calvine Fundi, **PhD**

JKUAT, Kenya

DEDICATION

This work is dedicated to my family; my wife Charity, my son Kirima and my daughters Linet and Viviane for their unconditional love, patience, understanding, spiritual and emotional support throughout the course of this thesis.

ACKNOWLEDGEMENTS

I would like to thank my supervisors, Dr. Kiroe and Dr. Ominde C. Fundi their guidance throughout this research and for all the help in and out of the lab. Your encouragement and constant checking on my work has made this work a great success. The work described in this document could never have been accomplished without your help, advice and guidance.

I would also like to acknowledge the help from Dedan Kimathi University of Technology, Mechatronic Engineering; Mr. Gichane, Mr. Nyaga and Mr Muriithi. Without your constant help you put for me to assist in programming lessons at no extra cost, this work would not have been completed. Many thanks to my friends and fellow master students at the control and instrumentation lab; Mr. Khata and Mr. Ayieko.

Thanks to all of you who played part in making my work a success.

TABLE OF CONTENTS

LIST OF TABLES

LIST OF FIGURES

LIST OF APPENDICES

LIST OF ABBREVIATIONS AND ACRONYMS

ADC	Analog to Digital Converter
ASICs	Application Specific Integrated Circuits
BMLD	Binaural Masking Level
Db	Decibels
DF	Dengue Fever
DHF	Dengue Hemorrhagic Fever
EEPROM	Electrically Erasable Programmable ROM
FFT	Fast Fourier Transform
FPG	Field Programmable Gate
GUI	Graphical User Interface
IC	Integrated Circuit
ICSP	In-Circuit Serial Programming
IDE	Integrated Development Environment
KEMRI	Kenya Medical Research Institute
LCD	Liquid Crystal Display
LED	Light Emitting Diode
ppm	parts per million
PWM	Pulse-Width Modulation
RAM	Random Access Memory
ROM	Read Only Memory

RTC	Real Time Clock
SAW	Surface Acoustic Wave
SD	Secure Digital
SRAM	Static RAM
USART	Universal Synchronous/Asynchronous Receiver/Transmitter
USB	Universal Serial Bus

ABSTRACT

The twenty first century has experienced swift changes in the development and advancement of different insecticide-based insect management tactics. This is with an aim of controlling diseases spread by various insects. One such disease is malaria caused by the plasmodium parasite spread through female mosquito bites. However, the current methods employed to control mosquito population in both private and public places are limited in various ways. First, aerosols have known health side effects to humans, and secondly, ultrasonic based systems emit low frequency waves known to have side effects on either hearing or human brain. In addition, these systems are considered inefficient as they are deployed indiscriminately. A more effective approach is to spray or activate the system when the target insect has been detected. In this research, an improved method of insect control is designed and implemented which involved a microcontroller-based system that is operational only when the target insect is within the effective detection zone. The detection of the insect is derived from processing of sound frequencies produced during insect flight using the Doppler effect and Fast Fourier Transform (FFT). These frequencies are recorded using a sound sensor (microphone system) that is connected to a micro-controller unit which is programmed using Arduino IDE platform to detect insects based on their sound, while the Python programming language was used in the frequency processing and GUI. Upon detection, a spray mechanism is activated to dispense the required insecticide. A sound generator was used to test the performance of the frequency detection system where the system was found to detect a broad frequency range with sufficient intensity. The system detected mosquito frequencies in the range of 434Hz and 496Hz, with a peak frequency of 465Hz. Other insects that was detected include horsefly, black-fly and tsetse fly at peak frequencies of 713Hz, 1178Hz and 1829Hz, respectively. This system is therefore effective in detection and control of these insects.

CHAPTER ONE

INTRODUCTION

1.1 Background of the study

Mosquitoes are vectors of causative agents for numerous diseases including, malaria, filariasis, dengue, Zika, chikungunya, and encephalitis. This ultimately result in approximately half a million to one million deaths annually and an enormous economic losses through the costs of vaccinations and vector controls as seen in the Zika virus outbreak in Latin America between 2015 and 2017, which cost approximately $18 billion (Cardé, 2015; O'Reilly *et al*., 2018).

Management of these diseases has posed a great challenge in recent times, mostly due to global warming, climate change and resistance to drugs. The main challenge is to find an efficient and affordable system that could be used to manage the mosquitos. Possible options being explored include mosquito control mechanisms such as: altering their breeding, destroying breeding grounds and mosquito repelling systems.

Recognition and classification of animals that use flapping fight, based on wing-beat frequency and other parameters, have become increasingly important in the automated identification of these groups. There is a demand for reducing insecticide use and not least to apply them with as little risk for non-target insects as possible. The key to reach this goal is to optimize the use of insecticides to periods and areas where pests are present and other insects are least affected. This inevitably involves recognition of the insects in the field (Kirkeby *et al*., 2021).

In chili fertigation farms, pests such as mites, snails, and maggots are a common type of pest that can be found in this farm by making the plants as their source of food and breeding ground. In this case, pest invasion is an unavoidable circumstance but can be controlled by having pesticide spraying periodically. Normally, the worker needs to manually spray the pesticide while wearing protective gear and walking from crop to crop. This method is indeed inefficient practice and hazardous chemicals used in spraying can

be fatal to the worker even wearing protective gear because research conducted found that the protective gears do not stop the chemical but only reduce the amount of exposure (Kassim *et al*., 2020).

The World Health Organization (WHO) estimates approximately 3 million cases resulting from pesticide poisoning happen every year, thus causing the death of 220,000 people who especially live in developing countries. Unregulated spraying during the disposition of the insecticide to the insects can lead to the low rate of coverage on insect body, wastage of insecticide and hazardous exposure to household members. With regulated spraying, a higher coverage of insecticide on an insect body is achieved, (Organization, 2020).

According to Kaczmarek and Niewiarowicz (2013), the velocity of a sound source with respect to an observer is a basic parameter which can describe motion. The Doppler effect is the best consequence of this. It is a change in the pitch of sound that occurs when a source of the sound is moving relative to a listener. Waves emitted from a moving source are perceived at higher or lower frequency by a stationary observer. The Doppler effect is applied in various instances, including, the tracking of weather storms, diagnosis of heart problems, radar communication, etc. By exploiting mosquito's wing beats and using the Doppler equation it is possible to calculate their buzzing sound and using the perceived sound to record the activity or passage of mosquitoes (Jean *et al*., 2018).

The aim of regulated insecticide spraying may not only be to achieve a higher insecticide coverage on insect body, but also to dispense the insecticide only to a target insect. One way to achieve the latter is by distinguishing insects by their wing beat frequencies. Following a study by Wang, Hu, Fu, Long, and Zeng (2017), wing beat frequencies play a significant role in insect behaviour. This is a natural phenomenon among mosquitoes where a male mosquito locates a female by the sound of their wing beats. According to Warren, Gibson, and Russel (2009), a female mosquito makes a higher pitched sound than its male counterpart by beating its wings up to 500-600 times per second and the male picks out the higher frequency of these beats when seeking a mate.

Using this principle, mosquito will be detected by their frequency range using frequency sensor to give an instantaneous analogue signal. The frequency signal is then fed into a micro-controller program to compare it with the known frequencies range data from Kenya Medical Research Institute (KEMRI) for the action to be triggered. If the detected frequency is found to be within the known range, a control mechanism shall be activated. This means, therefore, that the control mechanism shall be used only when necessary; hence, minimal usage of aerosols and other insect repellents with a guarantee that the mosquito will die.

According to Markus, (2017), the reason for existence of the Doppler effect is that when the source of the waves is moving towards the observer, each successive wave crest is emitted from a position closer to the observer than the crest of the previous wave. Therefore, each wave takes slightly less time to reach the observer than the previous wave. Hence, the time between the arrivals of successive wave crests at the observer is reduced, causing an increase in the frequency. While they are traveling, the distance between successive wave fronts is reduced, so the waves compress together (Aljalal, 2014). Conversely, if the source of waves is travelling away from the observer, each wave is emitted from a position farther from the observer than the previous wave, so the arrival time between successive waves is increased, reducing the frequency. The distance between successive wave fronts is then increased, so the waves retract out (Henderson, 2017).

Study by Amrani, (2013) argues that for waves that propagate in a medium, such as sound waves, the velocity of the observer and of the source are relative to the medium in which the waves are transmitted. The total Doppler effect therefore result from motion of the source, motion of the observer, or motion of the medium. For waves which do not require a medium, such as light or gravity in general relativity, only the relative difference in velocity between the observer and the source needs to be considered.

The Doppler effect also called the Doppler shift describes the frequency change of a wave in relation to an observer who is moving relative to the wave source. For example, the

change of pitch heard when a car sounding a horn approach and recedes from an observer. When compared to the emitted frequency, the perceived frequency is higher during the approach, identical at the instant of passing by, and lower during the recession (Wang, Hu, Fu, Long, and Zeng, 2017).

A summary work done by Roguin (2002) entails the noble work of Christian Doppler, who in 1842 hypothesized that sound frequencies change, relative to the observer, when emitted from a moving sound source. Doppler's hypothesis is demonstrated in an experiment involving an ambulance as a sound source, it is observed that as the ambulance approaches, the waves seem shorter, and the frequency becomes higher than when the ambulance moves away from a respective stationary listener. Much of this was experimented by Seddon and Bearpark (2003), in the analysis of inverse Doppler effect.

Equation 1.1 shows the formula for determining the observed frequency during the Doppler effect phenomena as the source moves towards the observer.

$$f_0 = \left(\frac{v}{v - v_s} \right) f_s \quad \text{..... (1.1)}$$

Where, f_0 is observed frequency, v is speed of sound in air, v_s is velocity of the source (negative if it's moving toward the observer), f_s is the emitted frequency of the source.

Once the ambulance passes the frequency of the sound decreases. The same equation is performed to determine the observed frequency, except in this case is positive. A similar change in frequency is observed if the observer is moving towards a stationary sound source. In this case the formula for determining the observed frequency of sound is given by Equation 1.2. The change in the equation is basically focusing on the parameter that describes the velocity of the receiver or the observer.

$$f_0 = \left(\frac{v + v_r}{v} \right) f_s \quad \text{..... (1.2)}$$

Where v_r is the velocity of the receiver, i.e. the observer (this is negative if the observer is moving away from the source).

We can also calculate the observed frequency if both the source sound and the observer are moving towards each other. In this case, the formula relating observed frequency and source frequency is given by Equation 1.3:

$$f_0 = \left(\frac{v + v_r}{v + v_s} \right) f_s \quad \text{..... (1.3)}$$

Sound waves seem to compress or elongate with moving sound source. Moving forward causing the waves in front to seemingly compress and waves in the back to seemingly elongate. The sound of an approaching ambulance siren will have a higher pitch than when it's moving away from you. This is a very practical by-product of sound physics. This Doppler effect enables one to know when to differentiate between an approaching ambulance and a retreating one and hence give way.

1.2 Statement of the problem

Mosquitoes are agents of numerous diseases that ultimately result in many deaths annually and huge economic losses through the cost of drugs. There are control systems that are available in form of bio-insecticides, electro-insecticides and ultra-sound repellents. However, these control systems have negative impacts like toxic residues in food, water, and air as well as effect on non-targeted organisms. For those repeatedly exposed, adverse health effects can include depression of the central nervous system and even permanent damage, as well as irritation of the eyes, lungs, liver and kidneys. In addition, over exposure to ultraviolet rays and ultrasound have known side effects to skin, human perception, and the brain at large. This research developed an insect control system based on Doppler effect as an improvement on the existing methods of mosquito control by implementing a spray mechanism that is operational only when the target mosquito is within the detection range. Detection is based on processing of sound frequencies produced during mosquito flight using Doppler effect and Fast Fourier Transform. This

system perform sound frequency processing using a microcontroller that is programmed to detect insects and activate spray mechanism only when necessary.

1.3 Justification

Detection of insects based on wing-beat frequencies allows the distinction between different types of insects. Tuning of the frequency detection system to respond to a specific frequency range ensures targeted control of a specific insect while avoiding exposure to non-targeted organisms. Activation of spray mechanism when a mosquito is within the range of the detection system reduces wastage of insecticides while ensuring efficient control of the insect, which also minimizes exposing humans to insecticides. Therefore, activation of spray mechanism of insect control system based on Doppler effect ensures efficiency in usage of insecticide thus minimizes the cost of expenditure in controlling of mosquitos.

1.4 Research objectives

1.4.1 General objective

The general objective of this study was to develop a cost-efficient insect control system based on Doppler sound effect principle.

1.4.2 Specific objective

This study was guided by the following specific objectives:

1. To implement a frequency detection method on a test control system for different frequency ranges.
2. To determine, through experimentation, the most appropriate frequency range for insect (mosquito) detection.
3. To validate performance of the insect detection technique.

CHAPTER TWO

LITERATURE REVIEW

Mosquito wing-beat frequency i.e., wing beat measurement has been experimented in different scopes and instruments for sound recordings. Examples include: Use of microphones to enable wide-spread acoustic mosquito surveillance and elimination (Gómez-Tejedor *et al*., 2014). In this piece of work, microphones were used as detectors/ receivers in the investigation of the sound frequencies in the location and elimination of the mosquitoes. Use of Doppler technique to identify mosquito species and the distance to the microphone has proven a possibility in experimental procedures such as in acoustic counting of mosquitoes in the field (Kim *et al*., 2021).

Kim *et al*., 2021 found that the wingbeat frequencies of individuals of *Culex quinquefasciatus* species of mosquitos did not vary, which remained relatively stable over time as shown in Figure 2-1. This trend of wingbeat frequencies of the same species of mosquito can be different from the wild strains because of a change in physical characteristics that can be due to changes in mass, wing area and wingspan of mosquitos.

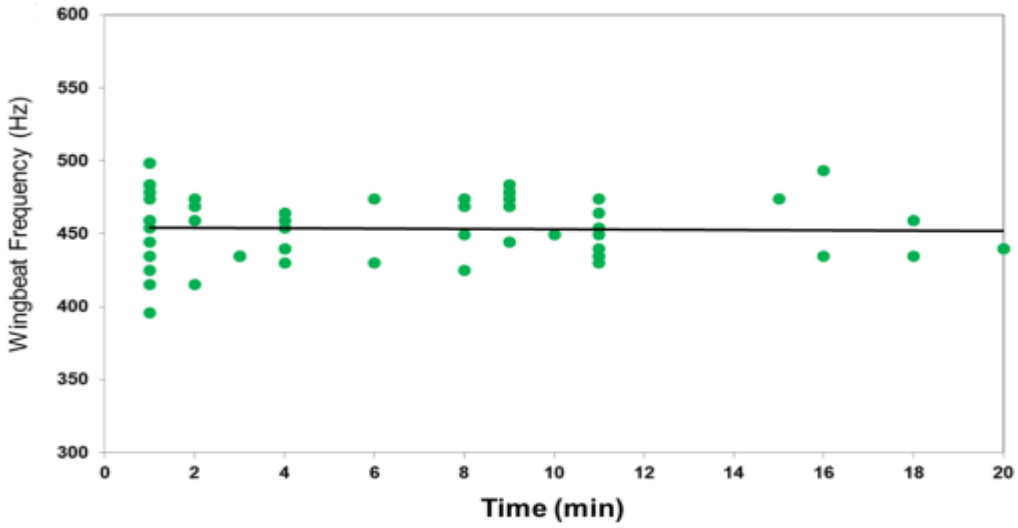

Figure 2-1: Wing beat frequency of mosquito showing changes in wingbeat frequencies over time (obtained from Kim *et al*., 2021)

Kassim *et al*., (2020) suggested that effective indoor residual spraying against malaria vectors depends on whether mosquitoes rest indoors i.e., endophilic behavior. This varies among species and is affected by insecticidal irritancy. Optimum effectiveness of insecticide-treated nets presumably depends on vectors biting at hours when most people are in bed. Time of biting varies among different malaria vector species, but so far there is inconclusive evidence for these evolving to avoid bed nets. They acknowledge that the use of an untreated net diverts extra biting to someone in the same room who is without a net. Oechslin, Neukom, and Bennet (2008) asserts that objects that are about to confront us are crucial for prospective actions. Even if we are not able to see what is approaching, the processing of auditory information enables us to identify the direction of moving sound sources. Various mechanisms allow us to accomplish this task most effectively. To date all of the mechanisms that have been widely discussed are based on sound-level differences or on timing aspects of incoming sounds.

Sound sources which move radially towards or away from the listener emitting signals with constant amplitudes. If objects are too far away from us to produce any perceivable level differences, this has to rely on other acoustic cues. In an experiment using synthesized sounds in a virtual environment, it was found out that the Doppler effect, which shifts the frequency of the direct sound and its reflections, is sufficient to identify correctly whether a moving sound source approaches or recedes (Oechslin, Neukom, and Bennet, 2008).

In psychoacoustic experiments, the subjects were presented with dichotic and diotic stimuli of a set of real-life recordings taken from a passing passenger car and then asked to determine the velocity of the object and its minimal distance from the listener (Kaczmarek and Niewiarowicz, 2013). The results allow us to separate monaural distance perception cues from binaural ones, and thus show that binaural cues contribute significantly to the perception of velocity. For short distances and high velocities, the presentation of binaural cues causes a decrease in the perceived velocity while for long distances and low velocities this causes a clear increase.

By estimating the minimal distance from the passing object, one observes a significant difference between dichotic and diotic presentation, which can be explained by an increased loudness of dichotic stimuli due to the Binaural Masking Level Difference (BMLD). Furthermore, it is shown that the main parameter for determination of distance is the maximum sound pressure level at the listener's position. However, dynamic cues e.g., change of sound pressure level over time and Doppler shift are of considerable importance for the plausibility of the auditory scene (Ma, Yang, and Nie, 2009). Gibson and Russell (2006), classified the reports that male mosquito feathers attract female mosquitoes. In Aedes aegypti and Aedes albopictus, 466 Hz and 462 Hz female mosquito frequency sounds generated respectively. From the experiments of Esch and Wilson, (1967), the sounds produced by the thoracic flight machinery of bees and flies appear to be composed of two main vibration modes. The lower frequency one corresponds to the wing beat frequency.

Fourier analysis of the sounds gives only harmonics of the wing beat frequency. However, oscillograms of the waveforms show that the higher frequency vibration is nearly independent of wing beat frequency. The high frequency vibration is probably important in bee communication. Speculation is that it is due to skeletal vibration which is relatively undamped by muscular and aerodynamic loading. Acoustic distortion in hearing organs exists usually as an interesting epiphenomenon.

Mosquitoes, however, appear to use wing beat frequency as a sensory cue that enables male–female pairs to communicate through a signal that depends on auditory interactions between them (Gibson and Russell, 2006). Frequency matching may also provide a means of species recognition. Morphologically identical but reproductively isolated molecular forms of Anopheles gambiae fly in the same mating swarms, but rarely hybridize. Extended frequency matching occurs almost exclusively between males and females of the same molecular form, suggesting that this behavior is associated with observed assortative mating.

Salim *et al*., (2017), asserts that the increasing cases of Dengue Fever (DF) and Dengue Hemorrhagic Fever (DHF) in the last decade have been reported worldwide. These conditions have led to huge economic loses and health complications. At present, no direct cure for DF and no efficient device to control or detect the Aedes mosquitoes that causes DF are available. Therefore, the fabrication of a device will reduce the probability of get infection since it works as a warning system, to exterminate Aedes mosquitoes as soon as discovered, and to evacuate the location until it be treated. Work by Salim *et al*., (2017), is the first to report the detection of the female Aedes mosquito in human habitations using a Surface Acoustic Wave (SAW) sensor. The feasibility of an acoustic-based device that records differences in signals and noise levels from different mosquito species has been demonstrated in instructing frequency differences to detect female mosquitoes. The SAW sensor response was investigated with simulated and real Aedes mosquito signals. Decreased resonant peak amplitude was obtained with different wing beat frequencies.

The magnitude was reduced by 0.6 dB and 1.25 dB with female and male Aedes mosquitoes, respectively. Furthermore, the SAW sensor exhibited good sensitivity in low sound pressure environments between 40 and 55 dB, making it suitable for use inside residential rooms. Hardy, Telfair, and Pielemeier, (1942), proposes that rigorous equation set up for the velocity of sound in gases can be used to calculate the velocity of sound in dry air at standard conditions from data taken in independent measurements. The result of this calculation is 331.45±0.05 m/s. An extensive survey of previous reported measurements has been made. After proper corrections are taken into account, the weighted mean is 331.464±0.05 m/s. The results of very precise interferometer measurements by the authors give 331.44±0.05 m/s.

Wong (1986), in his paper, describes the calculation of a new value for the speed of sound as 331.29 m/s in standard dry air at 0°C and at a barometric pressure of 101.325 kPa. The maximum uncertainty is estimated to be approximately 200 ppm. The theory of the calculation is based on the equation of state which is derived from published theoretical and experimental thermodynamic data on the constituents of the standard atmosphere.

Investigations which led to the general acceptance of the previous sound speed are examined, and there is good evidence to conclude that, in previous sound speed assessments, the maximum possible uncertainties were sufficient to encompass the above new sound speed. The variation of sound speed with carbon dioxide concentration and temperature is also discussed.

Aljalal (2014), applied a computer sound card and freely available audio editing software to measure accurately the speed of sound in air using the time-of-flight method. In addition to speed of sound measurement, inversion behavior upon reflection from an open and closed end of a pipe was demonstrated. The equipment needed was made readily available to any student with access to a microphone, loudspeaker and computer.

Amrani (2013), in their work compared the speed of sound measurement in air using two types of sensor that are widely employed in physics and engineering education, namely a pressure sensor and a sound sensor. A computer-based laboratory with pressure and sound sensors was used to carry out measurements of air through a 60 ml syringe. The Fast Fourier Transform (FFT) was used to find the fundamental frequency of the air column in the syringe, which can be used to calculate the sound speed for the sound sensor case. Meanwhile, for the pressure sensor case the time interval between the first peak and the nth peak of the periodic variation in pressure due to the sound wave travelling up and down the syringe was determined. The obtained average values of the sound velocity in air for the pressure sensor and the sound sensor were 340.9 ± 3 m/s and 346.7 ± 3 m/s, with errors of 0.6 % and 1.1 %, respectively, compared to the accepted value of 343 m/s at room temperature.

According to Unwin and Corbet (1984), the relationship between ambient temperature and wing-beat frequency in bees and flies of different sizes varies proportionally. The slope of the relationship changes with the size of the insect and was different for insects in hovering flight compared with individuals of the same species in forward flight.

In her research Pennycuick (1990), states that wingbeat frequencies were observed from the estimate of the power available from flight muscles, and an estimate of the power

required by an insect to fly. In their work, Moore, Miller, Tabashnik, and Gage, (1986) shows that a microcomputer-based instrument can be used to record and analyze flight movements of individual insects flying through a light beam. It is observed that small insects usually beat their wings at a higher frequency than large insects. For energetic reasons, the wing beat frequency is close to the natural resonant frequency of the wing movement.

With this review, the proposed study seeks to design an algorithm for instantaneous control of existing insecticides systems. The algorithm will be embedded in the system which will be integrated within the triggering mechanisms of the existing systems. By incorporating Doppler effect technique, the system will monitor the Doppler frequency from the approaching mosquito, this will be used to estimate the Doppler distance, which will then be compared to a preset value so as to trigger the spray mechanism in bio-insecticides or trigger ultrasound or ultra-violet light in electro-insecticides only when necessary.

According to Markus (2017), the reason for existence of the Doppler effect is that when the source of the waves is moving towards the observer, each successive wave crest is emitted from a position closer to the observer than the crest of the previous wave. Therefore, each wave takes slightly less time to reach the observer than the previous wave. Hence, the time between the arrivals of successive wave crests at the observer is reduced, causing an increase in the frequency. While they are traveling, the distance between successive wave fronts is reduced, so the waves compress together (Henderson, 2017). Conversely, if the source of waves is travelling away from the observer, each wave is emitted from a position farther from the observer than the previous wave, so the arrival time between successive waves is increased, reducing the frequency. The distance between successive wave fronts is then increased, so the waves retract out.

Study by Giordano (2009), argues that for waves that propagate in a medium, such as sound waves, the velocity of the observer and of the source are relative to the medium in which the waves are transmitted. The total Doppler effect therefore result from motion of

the source, motion of the observer, or motion of the medium. For waves which do not require a medium, such as light or gravity in general relativity, only the relative difference in velocity between the observer and the source needs to be considered.

CHAPTER THREE

METHODOLOGY

3.1 Overall design of insect control system

A laptop computer running on Windows 10 operating system with installations of Arduino Atmel® Studio 7 software are used to program Arduino UNO based on Atmega328P microcontroller. Arduino UNO board is programmed to read analog signals from microphone sound sensor and temperature sensor, display data over liquid crystal display (LCD), turn ON/OFF light emitting diodes (LEDs), and switch a spray mechanism depending on the detected sound frequency. Spray mechanism consist of a servo motor interfaced with a mosquito aerosol spray container such that one half of servo horn rests on the spray actuator. Microphone sound sensor is used to detect sound. Temperature sensor measure the temperature of the surroundings during experiments. The overall design block diagram of the insect control system is shown in Figure 3-1.

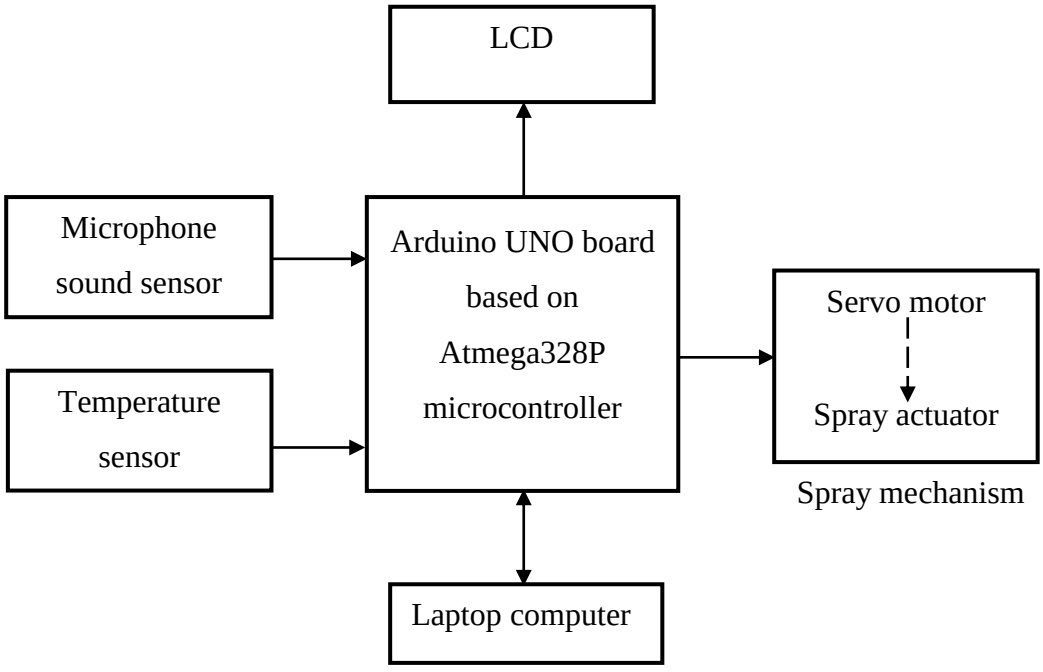

Figure 3-1: Block diagram of the insect control system

Signal flow between laptop computer and Arduino UNO board is bidirectional indicating programming and storage of data. Temperature sensor and microphone sound sensor provide input signals to Arduino UNO, denoted by unidirectional signal flow to Arduino UNO. Each component of the insect control system was chosen for this research based on their characteristics, availability and cost. The list below is the description of the components.

i. Arduino UNO based on Atmega328P microcontroller

Arduino UNO is an open source programmable board based on Atmega328 microcontroller that can be reprogrammed. The board contains 14 digital input/output pins, 6 analog inputs, one power jack, USB connector, one reset button, an In-Circuit Serial Programming (ICSP) header, a 16 MHz crystal oscillator, and other components. The function of all these components is to support Atmega328 microcontroller. The board is powered by a USB cable connected to a computer (which also functions as a serial communication between a computer and the board) or an external power supply. The recommended external supply voltage range is 7 to 12 volts, however, the operating voltage of microcontroller is 5V which is supplied from either a USB cable or a regulated supply or external power source.

The digital input/output pins (0-13) can function as input or output, which can be set by a program. Six of the 14 digital input/output pins of Arduino UNO board provide a pulse-width modulation (PWM) output, and can also provide analog output where the output voltage is adjusted according to a particular application. Analog output pin can be programmed between 0-255, representing a value of voltage between 0 and 5V. 6 analog inputs (0-5) can be used to read voltages from analog sensors. ICSP header allows the programming of microcontroller directly without using the bootloader. Otherwise, the bootloader allows uploading of a new code to the microcontroller through the USB cable connected to a computer. A reset button allows resetting the board so that program execution will start again. Arduino UNO based on Atmega328P microcontroller is shown in Figure 3-2.

Atmega328P is an 8-bit low power AVR microcontroller that is based on advanced Reduced Instruction Set Computer (RISC) architecture. It consists of a 32 Kb in-system self-programmable (ISP) flash memory, 1 KB electrically erasable programmable read-only memory (EEPROM), 2 KB Static RAM (SRAM), a 16MHz clock, 23 general purpose input/output pins, 32 general working registers, among other features. It has 6-channel 10-bit analog to digital (ADC) that convert analog to digital signals from the corresponding analog inputs. The programs and system development tools that support Atmega328P microcontroller include, C compilers, evaluation kits, macro assemblers, in-circuit emulators and program debugger/simulators.

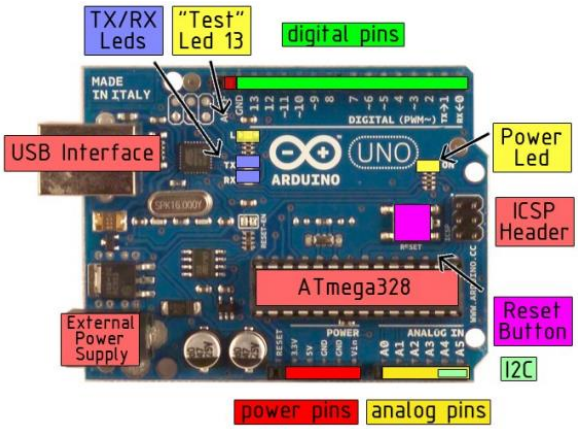

Figure 3-2: Arduino UNO based on Atmega328 (obtained from Arduino datasheet)

Atmel® Studio version 7.0 is an integrated development platform for the development and debugging of AVR microcontroller program applications. The software supports programs written in C, C++ and assembly languages with integrated compiler. It also supports importing Arduino IDE sketches into the platform as C/C++ projects. The software additional features include, support for more than three hundred AVR and ARM-based-devices, an integrated editor, provision of interface to in-circuit debuggers and programmers, and a vast source code library. Figure 3-3 show Atmel Studio 7 software used to program Arduino UNO based on Atmega328P microcontroller, showing a section of the code and a solution explorer displaying the list of libraries created and used in the program code.

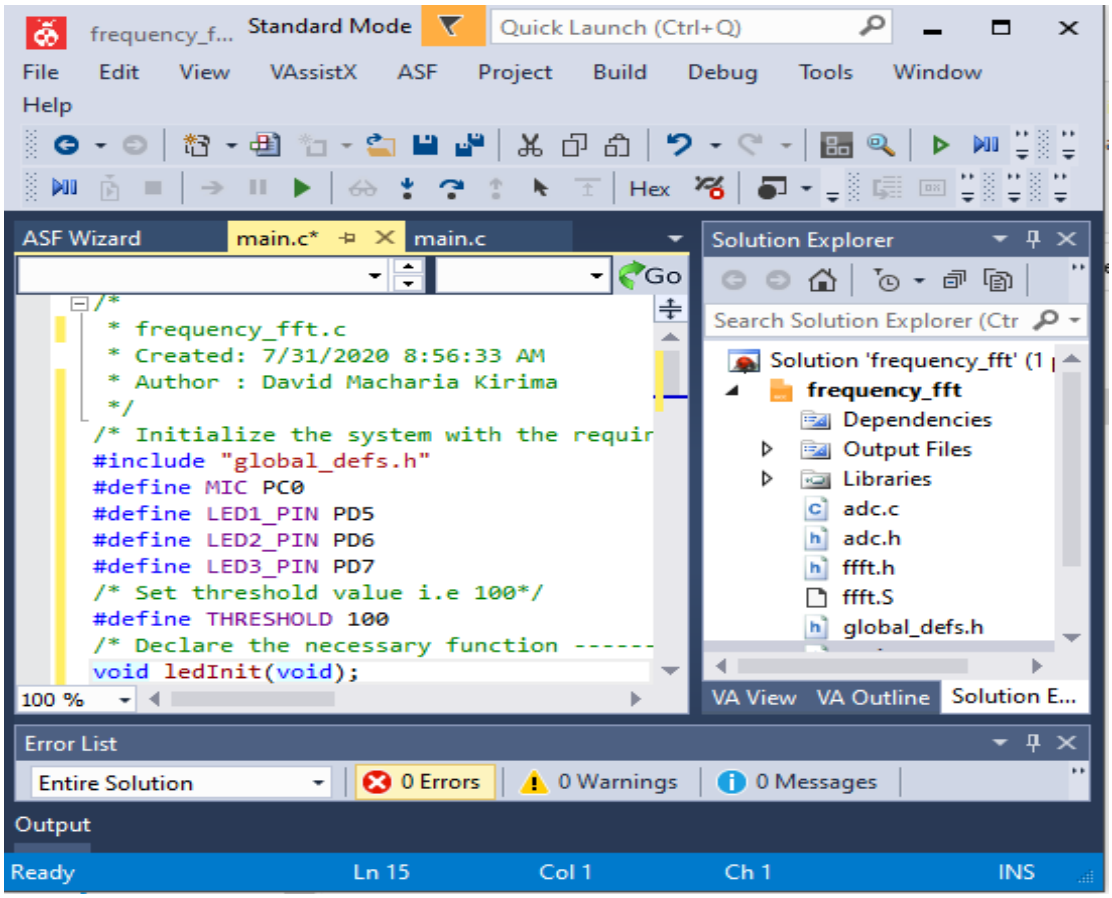

Figure 3-3: Atmel Studio 7 software

ii. Microphone sound sensor

Microphone sound sensor module incorporates a microphone and a processing circuitry, consisting a voltage comparator integrated circuit (IC), resistors, status LED and a potentiometer, which convert sound waves into electrical signals. LM393 comparator IC compare input voltage to the module and the output of the microphone, thus converting analog signal from a microphone sensor to digital output. The potentiometer is used to set the sensitivity of the module. The microphone functions as an acoustic sensor that convert sound waves into electrical signals. Condenser microphone contains two charged metal plates (a diaphragm and a back plate) forming a capacitor whose electrical capacitance C is given by equation 3.1.

$$C = \frac{\varepsilon A}{4\pi(D + \varepsilon d)} \quad \text{..... 3.1}$$

Where D is the foil thickness, A is the area of the diaphragm, d is air layer between two plates, and ε is the dielectric constant of the foil. An incident sound wave to the microphone cause a motion of the diaphragm resulting in vibrations with subsequent excitement from sound waves, which change the spacing between the diaphragm and back plate. This movement cause changes in the electrical signal that correspond to the sound detected by the microphone. Electrical signals is processed by LM393 op-amp IC, which output a signal voltage corresponding to the sound wave detected by the microphone.

Output signal of the sound sensor is a variation of signal's amplitude with time. However, determination of wing beat frequencies of mosquito require knowledge of the frequency contents of sound sensor output signals. These signals are then further processed to observe the frequency contents of the sound signal using Fast Fourier Transform (FFT). A FFT algorithm is thus implemented by a programming software in a laptop computer to transform the signals in time domain into energy distribution in frequency ranges to observe each frequency component of a sound wave. Each frame of the signal is transformed and further multiplied by a Hamming window to obtain a corresponding frequency spectrum. This implementation is defined by equation 3.2.

$$x_a = \sum_{n=0}^{N-1} x(n) e^{-j2\pi k/N}, \quad 0 \le k \le N \quad \text{..... 3.2}$$

Where $x(n)$ is the input data sequence and N denotes the elements of x. Figure 3-4 shows the microphone sound sensor module used to detect wing-beat sound frequencies of a mosquito.

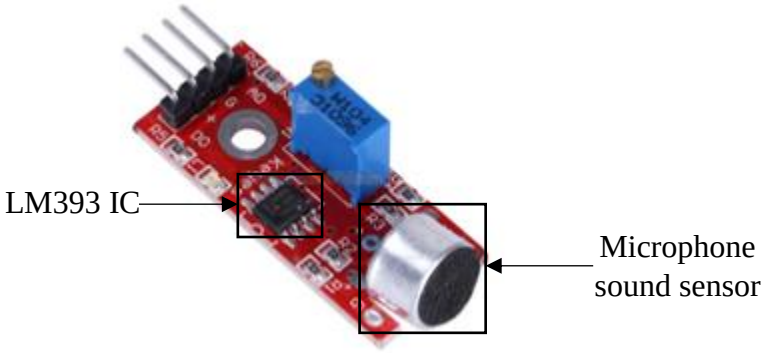

Figure 3-4: Microphone sound sensor module

iii. Servo motor

The Servo motor is a rotary actuator that allows for precise control of angular position which makes them suitable for use in closed-loop systems where precise position control is needed. Servo motors are part of a closed-loop system as shown in Figure 3-5, and they are a self-contained electrical device that rotate parts of a machine with high efficiency with great precision. Servo Motors are made up of: Control Circuit, Small DC Motor, and potentiometer. In this research, the servo motor was used to push and activate the aerosol container with great precision.

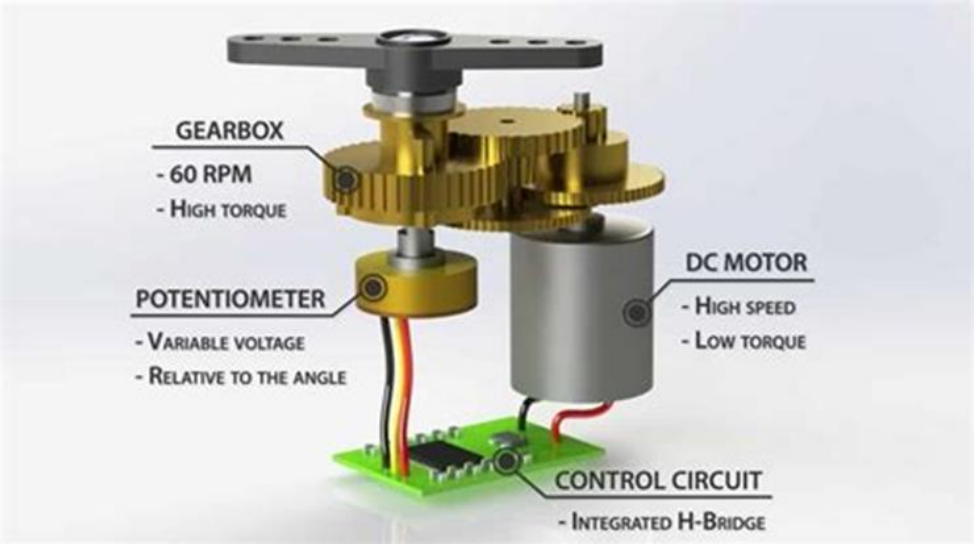

Figure 3-5: Servo motor

iv. Temperature sensor

LM35 temperature sensor is an integrated analog temperature sensor whose electrical output is proportional to Degree Centigrade. LM35 sensor does not require any external calibration or trimming to provide typical accuracies. The LM35's low output impedance, linear output, and precise inherent calibration make interfacing to readout or control circuitry especially easy. The main advantage of LM35 is that it is linear i.e. 10 mV/°C which means for every degree rise in temperature the output of LM35 will rise by 10 mV. Figure 3-6 shows LM35 sensor used to sense the temperature of the surrounding when the research experiments were being performed.

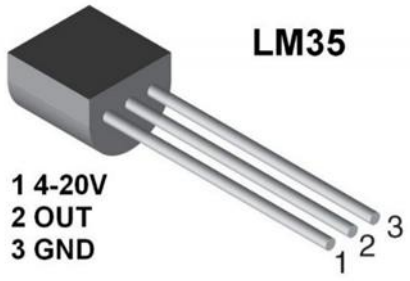

Figure 3-6: LM35 temperature sensor showing pinout functions

3.2 Schematic design of insect control system

Proteus version 8.9 software is used to design insect control schematic, where each component must be in the Proteus library before being available for selection. Arduino is programmed to read analog signals from sound sensor module and convert into frequency measurements and amplitude. Arduino sends a digital HIGH signal to a corresponding LED depending on whether sound frequency falls in which range among the four ranges chosen for this research. A servo motor is connected to a digital pin in order to receive digital signal from Arduino whose status depend on the frequency amplitude of the measured sound frequency. Servo motor rotating part presses against the nozzle of the insecticide aerosol spray container. LCD is connected to Arduino in 4 bit mode where

LCD data pins D4-D7 are used. The design of the insect control system is shown in Figure 3-7.

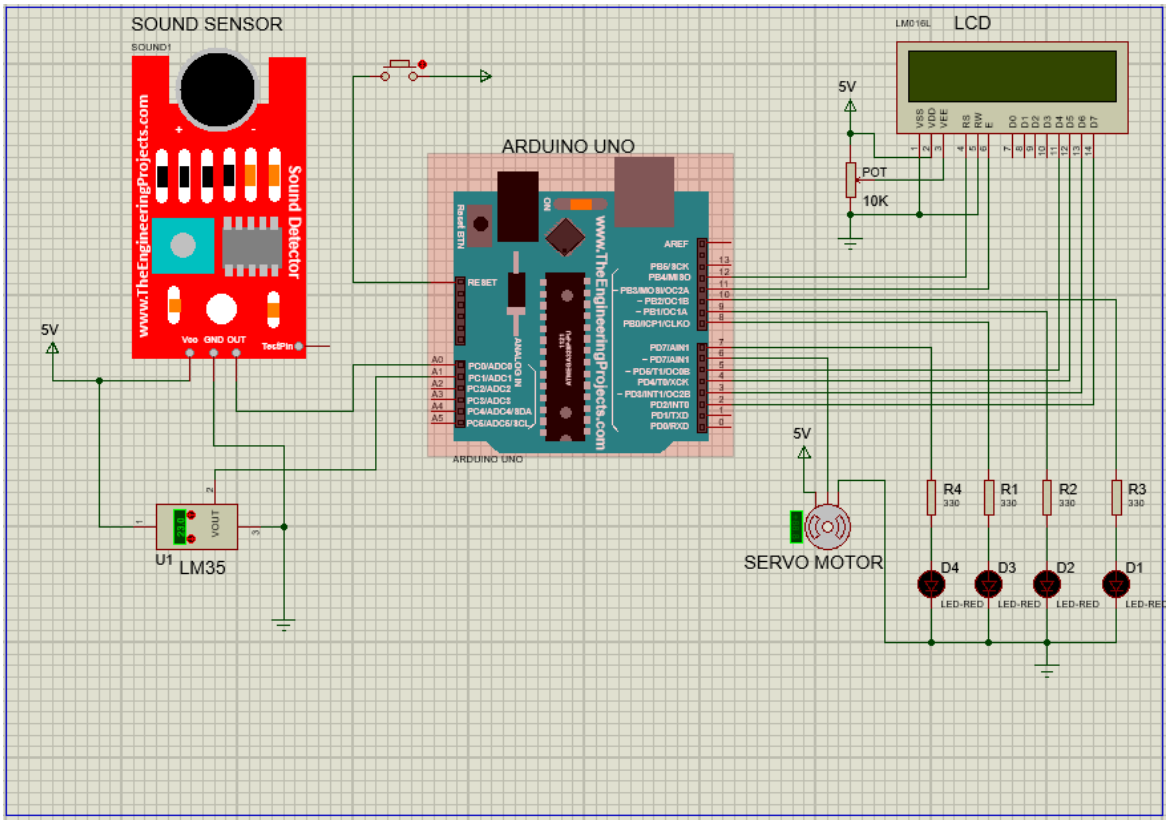

Figure 3-7: Circuit schematic diagram of insect control system

3.3 Experimental setup

3.3.1 Implementation of insect control system hardware

Once the circuit was designed, a prototype was then implemented in a circuit on a breadboard. LCD display was used alongside four LEDs to indicate detected insect type depending on a value of measured frequency falling in which frequency range. This indication provided a simple way to know the frequency range of a detected sound frequency. Servo motor and an insecticide aerosol can were placed in fixed positions such that the servo horn connected to servo motor output shaft rested on top of actuator. Upon triggering servo motor, servo horn rotated in a direction that pressed the actuator to spray

insecticide through the nozzle. Servo motor rotation angle is set in the Arduino sketch uploaded to the microcontroller. The whole circuit implemented on a breadboard is shown in Figure 3-8 alongside a laptop computer and the spray mechanism.

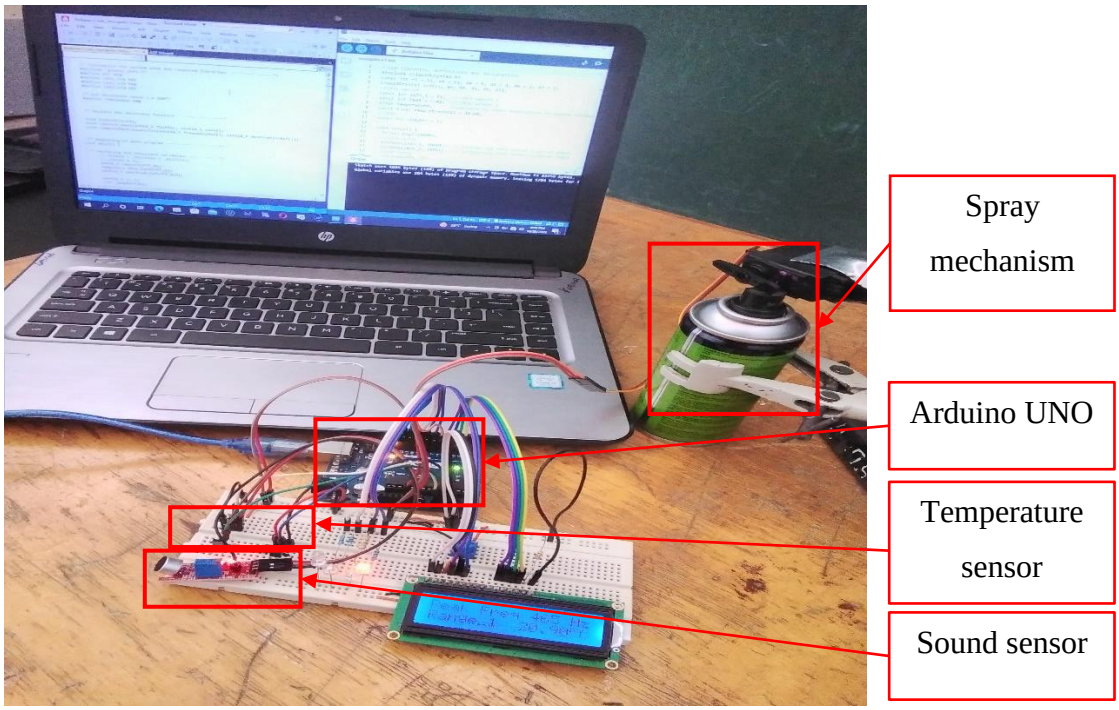

Figure 3-8: Photo of implemented insect control system circuit

3.3.2 Implementation of insect control program code

A control program for the system was implemented in Atmel® Studio 7, and the program code uploaded to the system. Initialization entails declaration of global variables and inclusion of libraries for sound sensor module, LCD, servo motor and USART communication. A program loop follows, which begins with checking of analog output signal of LM35 temperature sensor and subsequent conversion of the analog value to temperature measurement. Sound wave calculations are performed where Fast Fourier Transform (FFT) is used to convert the sound signals to spectral components that provides instantaneous frequency values. Peak frequencies corresponding to four frequency ranges are calculated from the frequency measurements, which are then displayed over LCD. Depending on the range category of a peak frequency, a corresponding LED is turned ON

to denote the frequency range of the peak frequency. If a measured peak frequency amplitude is above a threshold of 100 (indicating that a sound source is within 15 cm of a sound sensor), a spray mechanism is turned ON. Otherwise, it is turned OFF. The implemented algorithm flowchart diagram for the program is as shown in Figure 3-9. The actual program code is given in Appendix I.

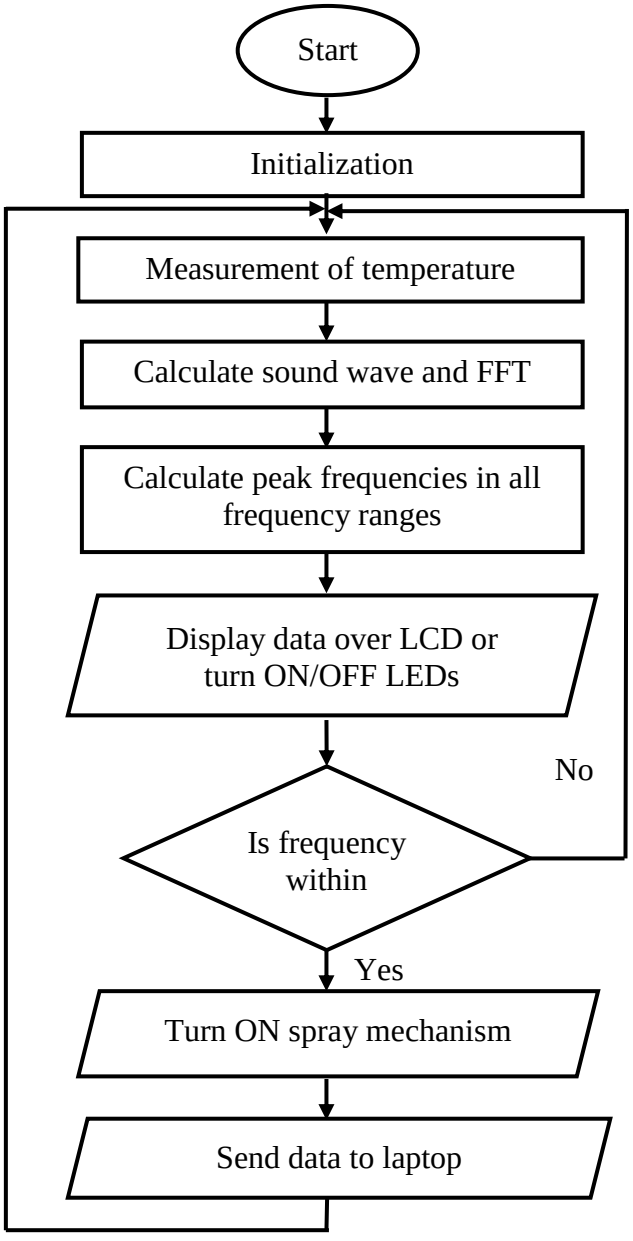

Figure 3-9: Program flowchart

3.3.3 Sound frequency generation setup

Function generator android app written by Keuwlsoft is used as a sound frequency generator. It is a dual channel function generator that outputs a waveform to audio output at 44.1 kHz having 16-bit resolution. Furthermore, it can generate sine, square and triangular waveforms in frequency range between 1 mHz and 22 kHz. The function generator app interface is shown in Figure 3-10a, which was used to generate sound waves of specific frequencies mimicking mosquito wing beat frequencies during performance testing of the insect control system.

Determination of frequency peak and range of mosquito can require using a mosquito for wing beat frequency measurement experimentation. A mosquito was captured in a sink in the laboratory and left unfed for a day. It was then placed within a mesh cage and an attractant, that is, glucose solution soaked in cotton wool, was positioned close to the insect control system to ensure the mosquito makes continuous flight in search of food as illustrated in Figure 3-10b. Sound waves produced by the flapping wings of a mosquito is measured by the microphone and converted to electrical signals, which are then transformed using FFT to the corresponding frequency components.

(a) **(b)**

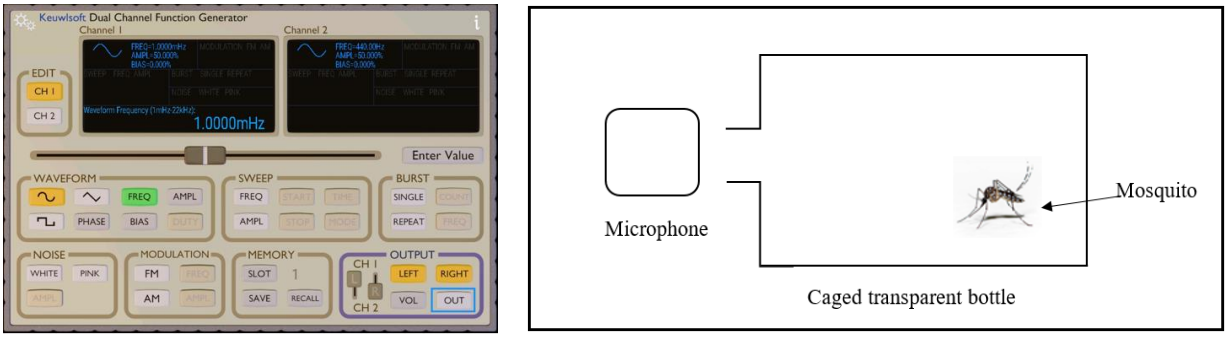

Figure 3-10: Sound frequency generator interface (a) and mosquito wing beat frequency experiment setup (b)

3.3.4 Sound frequency recording setup

A program code was written in Atmel® Studio 7 and uploaded to Arduino using a USB cable. Temperature and sound frequency measurements are sent to Atmega328P

microcontroller to the laptop computer through USART communication. A Frequency Plotter graphical user interface (GUI) written in Python programming language was used to receive any data made available in the USART port, which was connected to Arduino. Upon reception, the data was sorted and recorded on a .csv file based on the available sound frequency values. Figure 3-11 shows the implemented frequency plotter GUI, which require selection of port, sampling interval, samples per recording, cycle time, and output file name.

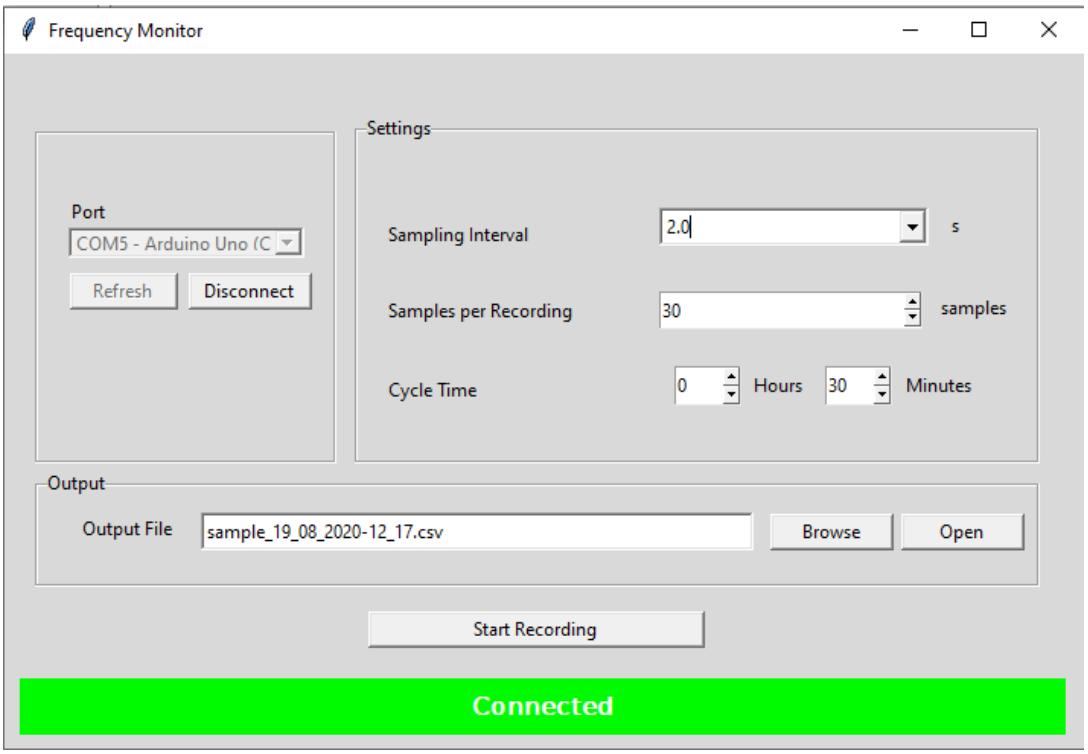

Figure 3-11: Frequency plotter

3.4 Testing the performance of insect control system

A range of test frequency bands with a specific frequency peak were selected as shown in Table 3-1. The sound frequency detection system was placed at a central position while a sound generator was used to mimic the sound produced by a flying insect, by setting it to a desired frequency range peak. A sound generator was then moved to simulate the flight of a flying mosquito within 15 cm radius around the detection system for a duration of 20

seconds. Afterwards, the frequency of the sound generator was changed to the next peak frequency, and the same procedure repeated for all frequency ranges. The sound detection system data was recorded for further analysis.

Table 3-1: Frequency reference table for performance tests

Serial No.	Frequency Peak	Frequency Range	Test duration (s)
1	450 Hz	425 - 475 Hz	20
2	500 Hz	475 - 525 Hz	20
3	550 Hz	525 - 575 Hz	20
4	600 Hz	575 - 625 Hz	20

3.5 Determination of appropriate frequency range for mosquito detection

To improve the overall performance of the insect control mechanism, it was required to validate the exact frequency range for a mosquito in order accurately detect it and dispense the insecticide appropriately. From the obtained KEMRI data, the suggested frequency range of a mosquito wing beat frequency is 250 Hz – 500 Hz. A test mosquito was used to measure the actual mosquito frequency detectable by the sound system. The technical challenge was to detect the whining noise more efficiently than the human ear, and separate it from ambient sounds such as human chatter. In practice it is quite difficult to record the sound of a mosquito in-flight in an open room. To mitigate this challenge, an enclosed experiment setup as shown in Figure 3-10b, was adopted. The mosquito was introduced to the above test setup and the wing beat sound recorded for 3 minutes, and further analyzed.

3.6 Validating the performance of insect detection system

Once the test circuit was actualized, tested and the mosquito frequency confirmed, a final test experiment was conducted to show the system could detect different types of insects concurrently. The detection mechanism involved reading the sound frequency and amplitude, from the sound sensor and determining whether the sound was within a predefined frequency range and the amplitude above a determined volume threshold. The volume threshold was related to the distance the insect was from the sound sensor. If the volume was above 100 units, the insect was within 15cm radius from the sound sensor i.e., the effective spray range of the insecticide.

Thus, sound received from the sensor had to have 2 properties: within the frequency range of interest and of sufficient volume magnitude i.e., greater than 100 units. When these 2 conditions were met, then it was resolved that a detection was made, and the system could activate the spray mechanism. Any sound signal within the insect range but below 100 volume units was considered that the insect was outside the insecticide effective spray range or background ambient noise. It is of point to note that the target frequency range and the threshold volume magnitude are adjustable and are the key variables used when adopting the system to counteract other target insects such as Horse fly, Black fly and Tsetse fly. These insects' sounds were simulated using a sound generator with the following frequencies: Horse fly – 713 Hz, Black fly – 1178 Hz, Tsetse fly – 1829 Hz. Once a detection was made it was indicated using LEDs and ON/OFF indicators in the frequency monitor. An example of the analysis graph is as shown in Figure 3-12.

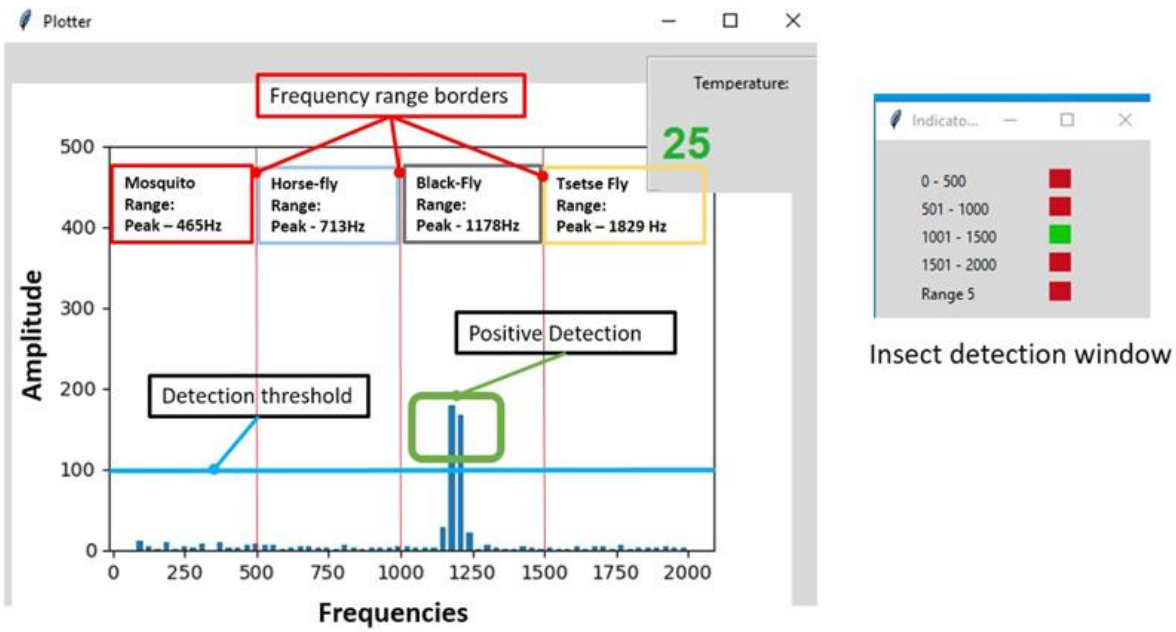

Figure 3-12: Graphical user interface showing FFT results for different frequency ranges and the detection indicator window

CHAPTER FOUR

RESULTS, ANALYSIS AND DISCUSSION

4.1 Results

4.1.1 Initial sound sensing performance test

The sound test experiment was performed, and the results recorded in the format show in Table 4-1. Due to the large size of the raw data, a sample of the obtained data during a performance test in 403Hz to 651Hz range is as shown in Table 4-2. Sound frequency generator was used to generate frequencies in the in the range of 93Hz to 1984Hz. During the conversion of sound waves into spectral components using Fast and Fourier Transform (FFT), a series of frequencies between 93Hz and 1984Hz range were calculated and recorded as column headings in an excel file. Frequency amplitudes of each sound frequencies measured every 3 seconds were recorded in corresponding frequency value column. The cells color coded to denote the magnitude of frequency amplitudes indicated at a glance frequencies with higher amplitudes, shown by cells colored in green. Amplitude equal to or greater than a value of a hundred corresponded to when sound source within 15 cm from a sound sensor.

Table 4-1: Mosquito frequency data collection table

Date	Time	Temperature	Amplitude for given frequencies

Table 4-2: Sample results of sound sensing performance test

Date	Time	Temp	403 Hz	434 Hz	465 Hz	496 Hz	527 Hz	558 Hz	589 Hz	620 Hz	651 Hz
19/08/2020	13:20:35	22	68	65	16	51	101	83	11	25	26
19/08/2020	13:20:38	21	31	12	22	31	5	13	10	2	1
19/08/2020	13:20:41	21	0	7	5	3	5	3	5	7	2
19/08/2020	13:20:45	21	12	5	4	8	20	4	1	5	8
19/08/2020	13:20:48	21	5	9	7	8	8	4	7	2	2
19/08/2020	13:20:52	22	6	4	11	4	11	1	5	2	4
19/08/2020	13:20:55	22	4	5	5	7	6	2	5	1	4
19/08/2020	13:20:58	22	0	3	15	12	5	7	8	8	1
19/08/2020	13:21:02	21	1	5	14	6	4	2	6	5	6
19/08/2020	13:21:05	22	3	11	35	31	2	1	5	3	5
19/08/2020	13:21:09	22	4	8	24	21	12	9	11	6	8
19/08/2020	13:21:12	21	10	1	16	12	2	4	1	10	5
19/08/2020	13:21:16	22	5	1	23	7	3	11	5	10	5
19/08/2020	13:21:19	22	5	18	71	51	4	4	4	3	6

Frequency magnitude variation during performance test is shown in a graphical plot of Figure 4-1.

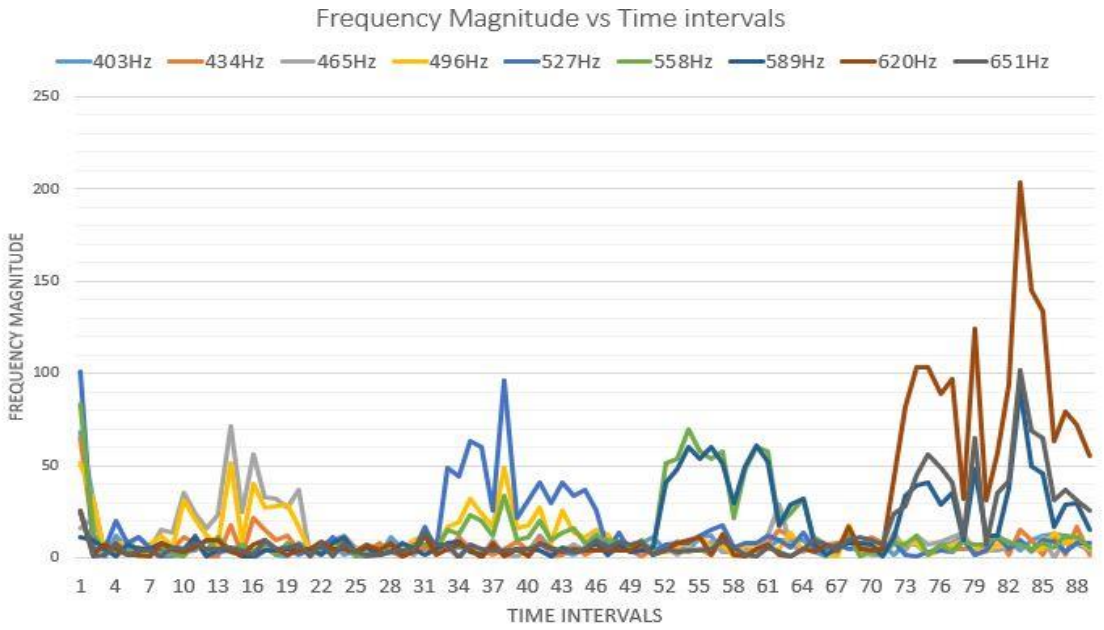

Figure 4-1: Frequency magnitude variation tests for different insects

As shown from the Figure 4-1, the frequencies and magnitudes of the generated sounds were accurately recorded by the sound sensing system. The figure is also color coded to enable easy distinction of areas with high magnitude denoted in green and areas with low magnitude denoted in yellow. An example is shown in Table 4-3.

Table 4-3: Magnitude scale coloring

Date	Time	Temp	403 Hz	434 Hz	465 Hz	496 Hz	527 Hz	558 Hz	589 Hz	620 Hz	651 Hz
19/08/2020	13:20:35	22	68	65	16	51	101	83	11	25	26
19/08/2020	13:20:38	21	31	12	22	31	5	13	10	2	1
19/08/2020	13:20:41	21	0	7	5	3	5	3	5	7	2
19/08/2020	13:20:45	21	12	5	4	8	20	4	1	5	8

Cells with low magnitude values – colored yellow

Cells with high magnitude values – colored green

4.1.2 Determination of the appropriate frequency range for mosquito detection

Once the sound sensing system was successfully tested, the second mosquito frequency confirmation test was then performed. Based on KEMRI data, a mosquito's wing beat frequency should range between 250 – 500Hz. Since this is a wide frequency range, an experiment was conducted to narrow the frequency range and confirm whether the mosquitoes used in the research produced sound within the recommended frequency range. The test was followed as described in section 3.5 and is summarized as follows: a mosquito was placed within the mesh cage and an attractant (i.e., glucose solution soaked in cotton wool) was positioned close to the sound recording device to ensure that mosquito flight in search of food. Due to the large size of the raw data, a sample of the obtained results is as shown in Table 4-4.

Table 4-4: Sample results of mosquito wing-beat frequencies

Date	Time	Temp	310 Hz	341 Hz	372 Hz	403 Hz	434 Hz	465 Hz	496 Hz	527 Hz	558 Hz
19/08/2020	12:17:45	20	8	2	9	6	4	14	5	4	10
19/08/2020	12:17:51	20	20	10	59	70	15	38	100	100	34
19/08/2020	12:17:57	20	0	0	2	0	2	0	4	0	0
19/08/2020	12:18:03	20	4	5	5	4	5	3	5	1	3
19/08/2020	12:18:09	20	4	4	4	3	82.5	232.5	135	2	4
19/08/2020	12:18:15	20	17	3	4	22	87.5	237.5	137.5	3	3
19/08/2020	12:18:21	20	26	2	9	8	65	205	112.5	26	7
19/08/2020	12:18:27	20	24	19	11	8	80	192.5	110	3	2
19/08/2020	12:18:33	20	26	100	92	45	55	175	75	9	12
19/08/2020	12:18:39	20	26	4	24	24	60	235	117.5	6	5
19/08/2020	12:19:45	21	7	7	5	3	70	210	117.5	4	0
19/08/2020	12:19:51	20	7	4	3	5	75	225	132.5	1	4
19/08/2020	12:19:57	20	15	5	13	8	70	210	115	0	7
19/08/2020	12:20:03	20	9	31	34	9	67.5	202.5	105	4	3
19/08/2020	12:20:09	21	4	4	5	5	5	5	8	5	4
19/08/2020	12:20:15	21	5	2	5	3	5	4	3	5	3

The collected data was used to plot variation of amplitudes of each of the measured frequencies as shown in Figure 4-2. The detected mosquito frequencies are 372Hz, 403Hz, 434Hz, 465Hz, 496Hz, 527Hz, and 558Hz. Variation was due to the variation of wing-beat frequency variation as mosquito flapped its wings inside the cage.

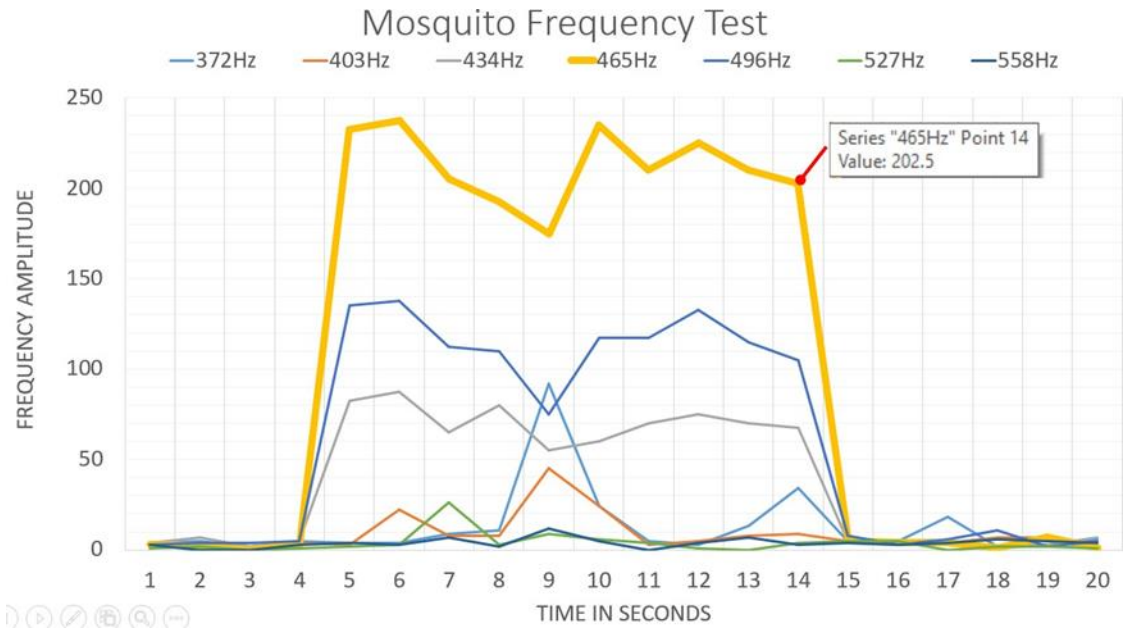

Figure 4-2: Frequency variation test of mosquito

4.1.3 Performance experiment for mosquito and other insects

With the successful completion of the 2 initial tests, a final experiment was conducted. This experiment involved the simulation of different insect frequencies while mimicking the path of a flying insect. The selected frequencies for simulation included: Mosquito - 465Hz, Horse fly – 713Hz, Black fly – 1178Hz, Tsetse fly – 1829Hz. The experiment procedure was followed as described in section 3.6 and is summarized as follows: These frequencies were simulated for a period of approximately 300 seconds. The frequencies were simulated one after the other and the data collected. The main objective of the test was to observe whether the system would be able to distinguish between different types of insects and once an insect is detected, the insecticide was to be dispensed which was illustrated using the lighting of an LED. Due to the large size of the raw data, a sample of the obtained results is as shown in Table 4-5.

Table 4-5: Sample results of different insects' simulation experiment

Time	403Hz	434Hz	465Hz	496Hz	527Hz	651Hz	682Hz	713Hz
18:48:26	7	28	26	4	10	5	3	7
18:48:32	7	14	35	14	5	5	10	4
18:48:38	1	73	103	32	4	2	4	3
18:48:44	4	53	95	21	0	2	1	7
18:48:50	4	62	96	29	4	7	2	2
18:48:58	4	90	136	39	6	4	2	7
18:49:06	4	88	130	40	2	4	4	5
18:49:12	8	86	138	35	2	4	1	2
18:49:19	8	82	140	41	6	1	5	4
18:49:25	7	84	131	28	2	5	4	7
18:49:31	10	81	137	34	8	5	3	3
18:49:36	5	83	135	37	3	1	9	2
18:49:41	5	80	114	36	1	4	1	1
18:49:47	4	4	6	2	4	4	3	4
18:49:51	6	2	6	2	3	5	3	7
18:49:58	4	6	0	4	6	1	0	2
18:50:05	4	4	4	4	4	9	190	276
18:50:11	5	6	1	8	4	7	140	185
18:50:18	4	4	3	4	4	8	189	263
18:50:25	5	4	4	7	5	11	178	244
18:50:33	9	4	4	6	7	7	173	238
18:50:38	4	10	1	9	1	6	208	280
18:50:45	6	2	3	2	5	20	191	268
18:50:52	0	4	0	4	2	19	221	311

Figure 4-3 shows the frequency magnitude versus the time in seconds for the different insect frequencies. The system detected the frequencies of the simulated wing-beat frequencies for mosquito, horse fly, black fly and tsetse fly at 465Hz, 713Hz, 1178Hz, and 1829Hz, respectively. Each frequency was tested with the sound generator within 15 cm from a sound sensor.

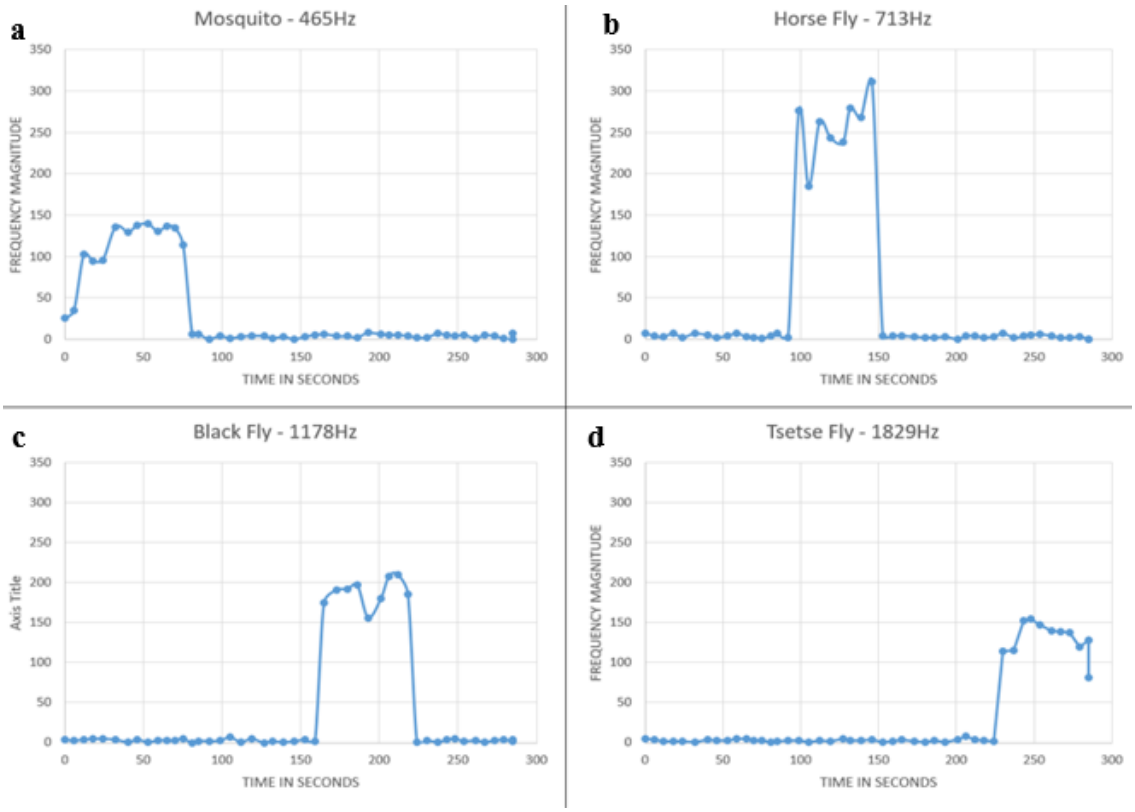

Figure 4-3: Relationship between frequency and distance for (a) mosquito, (b) horse fly, (c) black fly, and (d) tsetse fly

4.2 Data analysis

Performance test results were analyzed and used to fine-tune the final detection mechanism to improve its accuracy. The data analysis methods and techniques included plots and graphs generated using a frequency plotter and Microsoft excel. The frequency plotter was connected directly to the micro-controller serial communication port to provide real-time visualization of the detected sound frequencies. The results from the various test experiments are presented in the sections below beginning with the initial sound sensing performance test, mosquito frequency range confirmation test and final performance experiment for the different types of insects i.e. Mosquito – 465 Hz, Horse fly – 713 Hz, Black fly – 1178 Hz, Tsetse fly – 1829 Hz.

The sound generator test frequencies were divided into 4 frequency bands with Peak frequencies of 465Hz, 527Hz, 558Hz and 620Hz as shown in Figure 4-4. The variation in frequency magnitude was attributed to the simulation of insect flight motion by changing the distance between the sound generator and the sound sensing module. From the result analysis, it was concluded that the sound sensor could detect sound from a broad frequency range with sufficient intensity. In addition, sound produced within a particular frequency range, was not detected in other frequency ranges. This showed successful attainment of the system performance requirements.

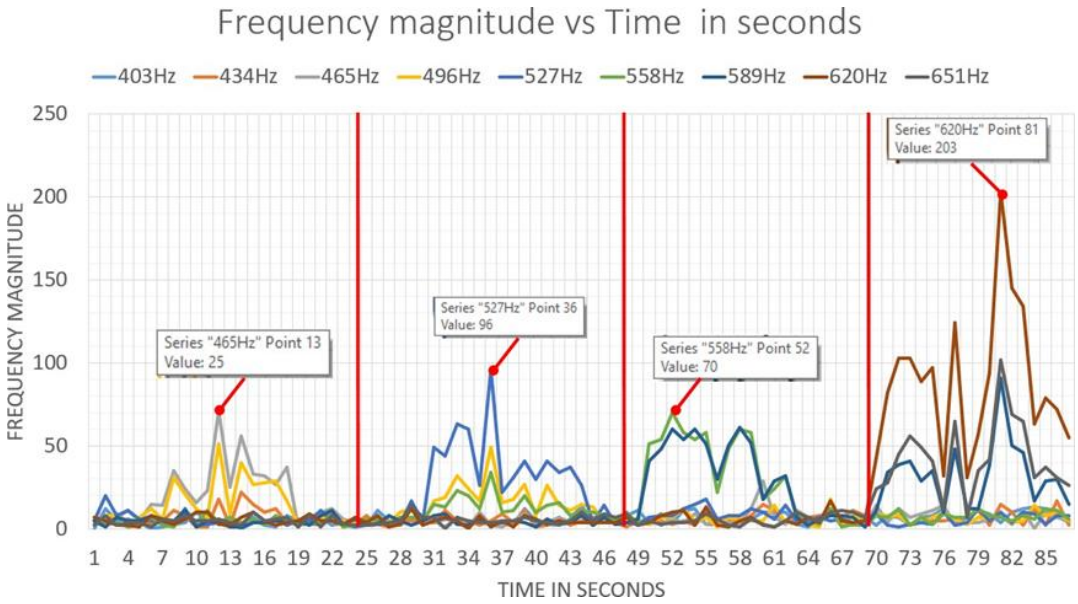

Figure 4-4: Frequency magnitude variation showing peak frequencies measured

From the graph shown in Figure 4-2, the mosquito produced frequencies between 434 – 496 Hz, with peak magnitude (deepest green shown in Table 4-4) obtained at 465 Hz with amplitudes greater than 100. This frequency was found to be within the recommended range by KERMI research data and thus showed the sound sensing module and captures mosquitoes adhered to the required standard.

Figure 4-5 shows the actual GUI recording during the detection process for the different insect sound frequencies. As illustrated when a sound profile fell within a particular frequency range and had a magnitude above 100 units, a detection was recorded as

indicated in the LED window shown to the side. From the graphs it was evident that successful detection was achieved for the different types of insects. This illustrated that the system was able to distinguish different types of insects and send the appropriate signal for the actuation of the insecticide. The results also showed that when a sound source was close to the sound sensor, the magnitude of the frequency was high thus a negative gradient correlation. This established a relationship between Doppler frequency and distance as illustrated by the speed of sound equation in air.

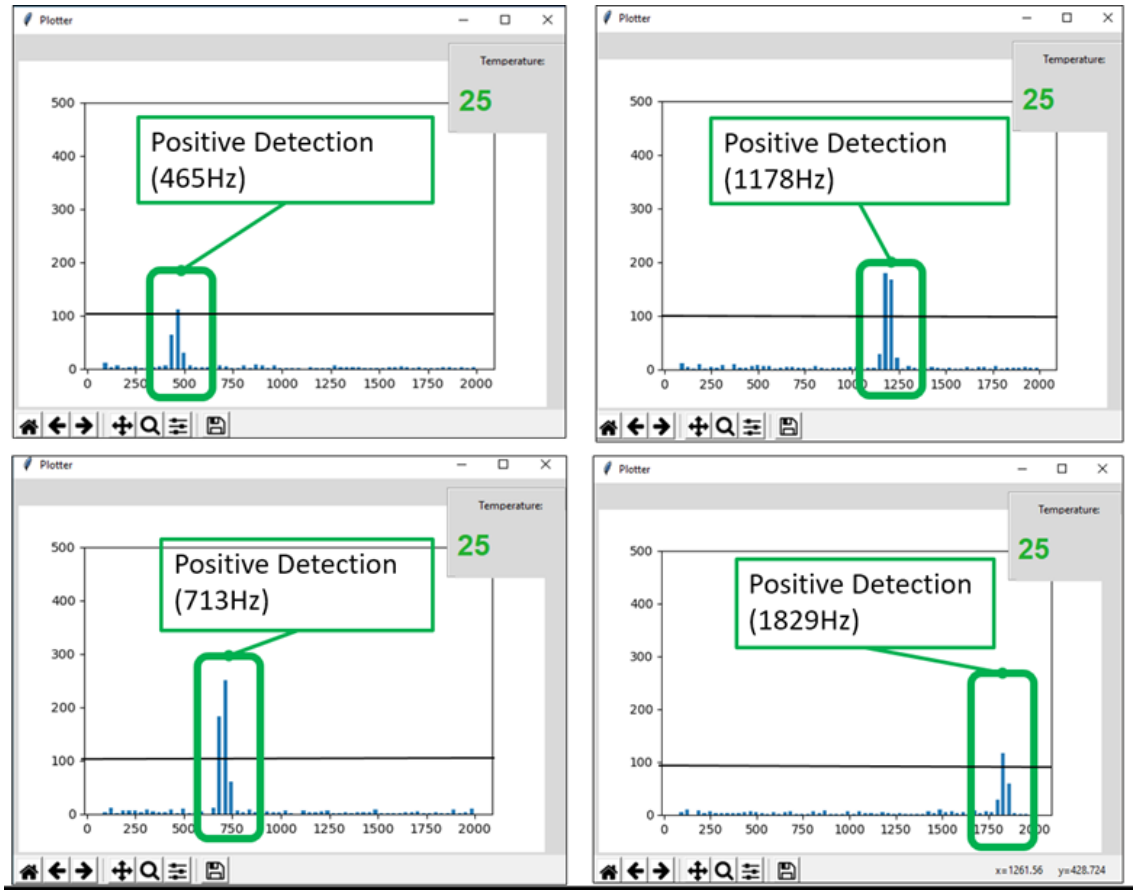

Figure 4-5: GUI showing positive detections for the various types of insects

CHAPTER FIVE

CONCLUSION AND RECOMMENDATION

5.1 Conclusion

The following conclusions were made from the study:

5.1.1 Determination of the most appropriate frequency range for mosquito detection

Through experimentation, the appropriate frequency for mosquito detection was found to be 250-500 Hz. This was used to trigger the switching mechanism to exterminate the mosquito.

5.1.2 Implementing the frequency detection method on a test control system for different frequency ranges

A frequency detection system was developed. The system was able to detect mosquito, horsefly, black-fly and tsetse fly.

5.1.3 To verify the insect detection performance through test experiments

Through tests experiment, it was observed that, the relay (LEDs) was triggered at frequencies based on the detected amplitude. The user could pre-set a specific frequency at which the control unit initiated an ON/OFF state i.e., HIGH state or LOW state. This in turn initiated either a spray mechanism or ultrasonic repellent.

A cost-efficient insect control system was designed and implemented. The system successfully detected different frequency ranges corresponding the sound made by different insects. From the actual experiment, Mosquito was detected at 465 Hz. Further, this research simulated other insects which included: Horse fly – 713 Hz, Black fly – 1178 Hz, Tsetse fly – 1829 Hz.

5.2 Recommendations

The following recommendations were made based on the findings of the study.

i. Refinement of the implemented circuit and addition of spray mechanism.
ii. Further experiments on other insect frequencies
iii. Mass production and testing of a final consumer product

REFERENCES

Ajel, A. R. (2021). Position and speed optimization of servo motor control through FPGA. *International Journal of Electrical & Computer Engineering, 11*(1), 319-327. doi:10.11591/ijece.v11i1.pp319-327

Aljalal, A. (2014). TIme of flight measurement of speed of sound in air with a computer sound card. *European Journal of Physics, 35*(6), 065008. doi:10.1088/0143-0807/35/6/065008

Amrani, D. (2013). A comparative study of sound speed in air at room temperature between a pressure sensor and a sound sensor. *Physics education, 48*(1), 65-71. doi:doi: 10.1088/0031-9120/48/1/65

Cardé, R. T. (2015). Multi-cue integration: how female mosquitoes locate a human host. *Current Biology, 25*(18), R793-R795. doi:10.1016/j.cub.2015.07.057

Esch, H., & Wilson, D. (1967). The sounds produced by flies and bees. *Zeitschrift für vergleichende Physiologie, 54*(2), 256-267.

Gibson, G., & Russell, I. (2006). Flying in Tune: Sexual Recognition in Mosquitoes. *Current Biology, 16*(13), 1311-1316. doi:10.1016/j.cub.2006.05.053

Giordano, N. (2012). *College Physics: Reasoning and relationships.* Cengage Learning.

Gómez-Tejedor, J. A., Castro-Palacio, J. C., & Monsoriu, J. A. (2014). Direct measurement of the speed of sound using a microphone and a speaker. *Physics Education, 49*(3), 310-313. doi:10.1088/0031-9120/49/3/310

Hardy, H. C., Telfair, D., & Pielemeier, W. H. (1942). The velocity of sound in air. *The Journal of the Acoustical Society of America, 13*(3), 226-233.

Henderson, T. (2017). The Doppler Effect--Lesson 3, Waves. *Physics tutorial. The Physics Classroom*.

Jean, P., de la Morena, D. L., Michanski, S., Tobón, L. J., Chakrabarti, R., Picher, M. M., . . . Moser, T. (2018). The synapric ribbon is critical for sound encoding at high rates and with temporal precision. *Elife, 7*, e29275. doi:10.7554/eLife.29275

Kaczmarek, T., & Niewiarowicz, M. (2013). Auditory motion perception in normal hearing and in hearing impaired people. *Acta Acustica united with Acustica, 99*(2), 283-291. doi:10.3813/AAA.918610

Kassim, A. M., Termezai, M. N., Jaya, A. R., Azahar, A. H., Sivarao, S., Jafar, F. A., . . . Aras, M. M. (2020). Design and development of autonomous pesticide sprayer robot for fertigation farm. *International Journal of Advanced Computer Science and Applications, 2*, 545-551. doi:10.14569/ijacsa.2020.0110269

Kim, D., DeBriere, T. J., Cherukumalli, S., White, G. S., & Burkett-Cadena, N. D. (2021). Infrared light sensors permit rapid recording of wingbeat frequency and bioacoustic species identification of mosquitoes. *Scientific Reports, 11*(1), 1-9. doi:10.1038/s41598-021-89644-z

Kirima, D. M., Kiroe, A., Ominde, C., & Khata, E. M. (2020). Development of a cost efficient insect control system based on Doppler sound effect principle. *International Journal of Science & Engineering Research, 11*(11), 444-449.

Kirkeby, C., Rydhmer, K., Cook, S. M., Strand, A., Torrance, M. T., J. L., . . . Græsbøll , K. (2021). Advances in automatic identification of flying insects using optical sensors and machine learning. *Scientific reports, 11*(1), 1-8. doi:10.1038/s41598-021-81005-0

Ma, L., Yang, J., & Nie, J. (2009). Doppler effect of mechanical waves and light. *Latin-American Journal of Physics Education, 3*(3), 550-552.

Markus, P. (2017). Waves, motion and frequency: the Doppler Effect. *Einstein Online, 5*(14), 1548-1550.

Moore, A., Miller, J. R., Tabashnik, B. E., & Gage, S. H. (1986). Automated identification of flying insects by analysis of wingbeat frequencies. *Journal of economic entomology, 79*(6), 1703-1706.

Oechslin, M., Neukom, M., & Bennet, G. (2008). The Doppler effect—an evolutionary critical cue for the perception of the direction of moving sound sources. *2008 international conference on audio, language and image processing*, (pp. 676-679). doi:10.1109/ICALIP.2008.4590253

O'Reilly, K. M., Lowe, R., Edmunds, W. J., Mayaud, P., Kucharski, A., Eggo, R. M., . . . Yakob, L. (2018). Projecting the end of the Zika virus epidemic in Latin America: a modelling analysis. *BMC medicine, 16*(1), 1-13.

Organization, W. H. (2020). *International code of conduct on pesticide management: guidance on management of household pesticides.* Food & Agriculture Org.

Panaligan, N., Cudera, L., Oda, J., & Amante, R. (2018). Android-based Agricultural Insect Trap Monitoring System Using Solar Panel and Arduino Technology. *Available at SSRN 3780518*, 18.

Pennycuick, C. J. (1990). Predicting wingbeat frequency and wavelength of birds. *Journal of experimental biology, 150*(1), 171-185.

Roguin, A. (2002). Christian Johann Doppler: the man behind the effect. *The British journal of radiology, 75*, 615-619.

Salim, Z. T., Hashim, U., Arshad, M. K., Fakhri, M. A., & Salim, E. T. (2017). Frequency-based detection of female Aedes mosquito using surface acoustic wave technology: Early prevention of dengue fever. *Microelectronic Engineering, 179*, 83-90.

Seddon, N., & Bearpark, T. (2003). Observation of the inverse Doppler effect. *Science, 302*(5650), 1537-1540.

Unwin, D. M., & Corbet, S. A. (1984). Wing beat frequency, temperature and body size in bees and flies. *Physiological Entomology, 9*(1), 115-121.

Wang, R., Hu, C., Fu, X., Long, T., & Zeng, T. (2017). Micro-Doppler measurement of insect wing-beat frequencies with W-band coherent radar. *Scientific reports, 7*(1), 1-8. doi:10.1038/s41598-017-01616-4

Warren, B., Gibson, G., & Russel, I. J. (2009). Sex recognition through midflight mating duets in Culex mosquitoes is mediated by acoustic distortion. *Current Biology, 19*(6), 485-491. doi:10.1016/j.cub.2009.01.059

Wong, G. S. (1986). Speed of sound in standard air. *The Journal of the Acoustical Society of America, 79*(5), 1359-1366.

Zhai, Y., Fu, S., Zhang, J., Lv, Y., Zhou, H., & Gao, C. (2020). Remote detection of a rotator based on rotational Doppler effect. *Applied Physics Express, 13*(2), 022012.

APPENDICES

Appendix I: System code

```
/*
 * frequency_fft.c
 * Created: 7/31/2020 8:56:33 AM
 * Author : David Macharia Kirima
 */
/* Initialize the system with the required libraries----------------*/
#include "global_defs.h"
#define MIC PC0
#define LED1_PIN PD5
#define LED2_PIN PD6
#define LED3_PIN PD7
/* Set threshold value i.e 100*/
#define THRESHOLD 100
/* Declare the necessary function ----------------*/
void ledInit(void);
void capture_wave(int16_t *buffer, uint16_t count);
void computeMaxFrequencies(uint16_t frequencyBuf[], uint16_t destinationBuf[]);
/* Beginning of main program --------------------*/
int main() {
```

```
	/* Declaring the necessary variables----------*/
	// TCCR1B = _BV(CS10) | _BV(CS11);
	// uint16_t t1;
	int16_t capture[FFT_N];
	complex_t bfly_buff[FFT_N];
	uint16_t spectrum_buf[FFT_N/2];
	uint16_t n, s;
	char tempBuf[16];
	uint16_t degBuf[2];
	uint16_t result;
	/* Functions to setu the LEDs, ADC and USART communication channels ----------*/
	ledInit();
	setupADC();
	USART_Init();
	while (1) {
		/* Reading and calculation of temperature from sensors ----------*/
		setupADC();
		degBuf[0] = readADC(1)*0.00763;
		degBuf[1] = readADC(2)*0.00763;
		result = (degBuf[0]+degBuf[1])/2;
```

```
/* Capturing of sound wave and calculate FFT----------*/
// TCNT1 = 0;
capture_wave(capture, FFT_N);
// t1 = TCNT1;
fft_input(capture, bfly_buff);
fft_execute(bfly_buff);
fft_output(bfly_buff, spectrum_buf);
/*-------- Calculate highest frequencies in 3 ranges ------*/
uint16_t highestFreqs[3] = {0};
computeMaxFrequencies(spectrum_buf, highestFreqs);
// Set LED1 State depending on 1st range----------------*/
if (highestFreqs[0] > THRESHOLD) {
        PORTD |= (1 << LED1_PIN);
        } else {
        PORTD &= ~(1 << LED1_PIN);
}
// Set LED2 State depending on 2nd range----------------*/
if (highestFreqs[1] > THRESHOLD) {
        PORTD |= (1 << LED2_PIN);
        } else {
        PORTD &= ~(1 << LED2_PIN);
```

```
}
// Set LED3 State depending on 3rd range----------------*/
if (highestFreqs[2] > THRESHOLD) {
        PORTD |= (1 << LED3_PIN);
        } else {
        PORTD &= ~(1 << LED3_PIN);
}
/*Transmission of fft through USART----------------*/
for (n = 0; n < FFT_N/2; n++) {
        s = spectrum_buf[n];
        memset(tempBuf, '\0', sizeof(tempBuf));
        sprintf(tempBuf, "%u", s);
        char *p = tempBuf;
        while (*p) {
                USART_Transmit(*p);
                p++;
        }
        USART_Transmit(',');
}
/*Transmission of temp through USART----------------*/
s = result;
```

```
                memset(tempBuf, '\0', sizeof(tempBuf));
                sprintf(tempBuf, "%u", s);
                char *p = tempBuf;
                while (*p) {
                        USART_Transmit(*p);
                        p++;
                }
                USART_Transmit('\n');
                // memset(data, '\0', sizeof(data));
                // sprintf(data, "%d samples in %u clocks", (int)FFT_N, t1);
                // sendString(data);
        }
}
/* End of main program -------------------------------------------------*/
/* Functions used within the program -----------------------------------*/
void ledInit(void) {
        DDRD |= (7 << DDD5);
        // DDRD |= (1 << DDD6);
        // DDRD |= (1 << DDD7);
}
void capture_wave(int16_t *buffer, uint16_t count) {
```

```
        ADMUX = _BV(REFS0)|_BV(ADLAR); //channel
        do {
                ADCSRA                                                  =
_BV(ADEN)|_BV(ADSC)|_BV(ADIF)|_BV(ADPS2)|_BV(ADPS1);
                while (bit_is_clear(ADCSRA, ADIF));
                *buffer++ = ADC - 32768;
                _delay_us(192); // Reduce sampling frequency to 4KHz from 18Khz
        } while (--count);
        ADCSRA = 0;
}
void computeMaxFrequencies(uint16_t frequencyBuf[], uint16_t destinationBuf[]) {
        uint16_t highestFreq = 0;
        for (int i = 0; i <= 20; i++) {
                if (frequencyBuf[i] > highestFreq) {
                        highestFreq = frequencyBuf[i];
                }
        }
        destinationBuf[0] = highestFreq;
        highestFreq = 0;
        for (int i = 21; i <= 40; i++) {
                if (frequencyBuf[i] > highestFreq) {
```

```
                highestFreq = frequencyBuf[i];
            }
        }
        destinationBuf[1] = highestFreq;
        highestFreq = 0;
        for (int i = 41; i <= 61; i++) {
            if (frequencyBuf[i] > highestFreq) {
                highestFreq = frequencyBuf[i];
            }
        }
        destinationBuf[2] = highestFreq;
}
```

Appendix II: Author's publications during MSc study

Kirima, D. M., Kiroe, A., Ominde, C., & Khata, E. M. (2020). Development of a cost efficient insect control system based on Doppler sound effect principle. *International Journal of Science & Engineering Research, 11*(11), 444-449.